

SENSOR AND ACTUATOR FAULT ANALYSIS IN ACTIVE SUSPENSION IN VIEW OF FAULT-TOLERANT CONTROL

Claudio Urrea and Marcela Jamett

Departamento de Ingeniería Eléctrica, Av. Ecuador 3519, Est. Central, Santiago, Chile

Keywords: Active suspension, sensor and actuator faults, full-vehicle suspension model.

Abstract: This paper shows the first step of a fault tolerant control system (FTCS) to control active suspension on a full-car suspension model. In this paper, the elimination of the inevitable pitch and roll actions of a spring suspension between each axle and the body of a vehicle is studied. An actuator (linear motor) producing an electromagnetic force and a pneumatic force acting simultaneously on the same output element is used. This linear motor acts as a force generator that compensates instantly for the disturbing effects of the road surface. Simulation results to illustrate the system's performance in front of the occurrence of sensor and actuator faults are shown.

1 INTRODUCTION

Vehicle suspension systems have developed over the last 100 years to a very high level of sophistication (Buckner, Schuetze, and Beno, 2000; Fukao, Yamawaki, and Adachi, 2000). Most vehicle today use a passive suspension system employing some type of springs in combination with hydraulic or pneumatic shock absorbers, and linkages with tailored flexibility in various directions. These suspension system designs are mostly based on ride analysis.

Traditionally automotive suspension designs have been a compromise between the three conflicting criteria of road holding, load carrying and passenger comfort. In fact, despite the wide range of designs currently available by using passive components, we can only offer a compromise between these conflicting criteria by providing spring and damping coefficients with fixed rates¹.

On the other hand, active suspensions have been extensively studied in the last three decades (Giua, Seatzu, and Usai, 2000; Lefebvre, Chevrel, and Richard, 2001; Lakehal-Ayat, Diop, and Fenau, 2002). In an active suspension the interaction between vehicle body and wheel is regulated by an actuator of variable length capable of supplying the entire control force system's requirements.

Ride comfort in ground vehicles usually depends

on a combination of vertical motion (heave) and angular motion (pitch and roll). Active suspension is characterized by a built-in actuator which can generate control forces to suppress the above mentioned roll and pitch motions.

Including the dynamics of the hydraulic system consisting of fluids, valves, pumps, etc., complicates the active suspension control problem even further since it introduces nonlinearities to the system. It has been noted that the hydraulic dynamics and fast servo-valve dynamics make controls design very difficult (Karlsson, Teely, and Hrovatz, 2001; Alleyne, and Hedrick, 1995). The actuator dynamics significantly change the vibrational characteristics of the vehicle system (Engelman, and Rizzon, 1993). Using a force control loop to compensate for the hydraulic dynamics can destabilize the system (Alleyne, Liu, and Wright, 1998). This full nonlinear control problem of active suspensions has been investigated using several approaches including optimal control based on a linearized model (Engelman, and Rizzon, 1993), adaptive nonlinear control (Alleyne, and Hedrick, 1995), and adaptive control using backstepping (Karlsson, Teely, and Hrovatz, 2001). These schemes use linear approximations for the hydraulic dynamics or they neglect the servo-valve model dynamics in which a current or voltage is what ultimately controls the opening of the valve to allow flow of hydraulic fluid to or from the suspension system. However, nowadays a novel family of highly dynamic electro-magnetic direct drives exist, *i.e.* servomotors

¹Components for passive suspension can only store and dissipate energy in a pre-determined manner.

that looks like a hydraulic piston with acceleration rates of over $200 [m/s^2]$ make cyclic movement at several Hertz possible.

Active suspension control systems reduce undesirable effects by isolating car body motion from vibrations at the wheels, but their component failures/faults are inevitable and unpredictable, and without careful and prompt treatment, they tend to develop into the severe total failure of the whole system. Continued operation of these systems has both economic and safety implications. Every mechanical system is vulnerable to faults that can lead to failure of the complete system, unless mitigating strategies are included at the design stage (Noura, Theilliol, and Sauter, 2000). Control element failures not only degrade the performance of control systems, but also may introduce instability and thus can cause serious operation and safety problems. Therefore, fault tolerance has been one of the major issues in process control.

In automated systems, the goal of the fault-tolerance is to continue operation in spite of failures, if this is possible. A general problem has been that fault conditions could not be treated as an integrated part of system design. Therefore, automated systems to provide uninterrupted service, even in the presence of failures are required (Zhang, Jiang, 2002).

Most of the past work uses the quarter-car model, which includes only two degree-of-freedom of the vehicle motion in the vertical direction (Lakehal-Ayat, Diop, and Fenaux, 2002). In general, the heave, pitch and roll motions are coupled and an impulse at the front or rear wheels excites all three motions. This means that pitch-, heave- and roll-controllers cannot be independently designed. Therefore, we take a model based in (Ikenaga, Lewis, Campos, Davis, 2000) including the full vehicle suspension dynamics considering heave, pitch and roll motions.

The paper is organized as follows: in section 2 the system description is given. In section 3, the state-space model for the full-vehicle suspension model is presented. In section 4, the vehicle controller is developed. Section 5 presents fault analysis and some simulation results. Finally, in section 6, the conclusions and outline future work are discussed.

2 SYSTEM DESCRIPTION

2.1 Full-Vehicle Suspension Model (Seven DOF System)

In this work, a full-vehicle suspension mathematical model depicted in Fig.1 is considered.

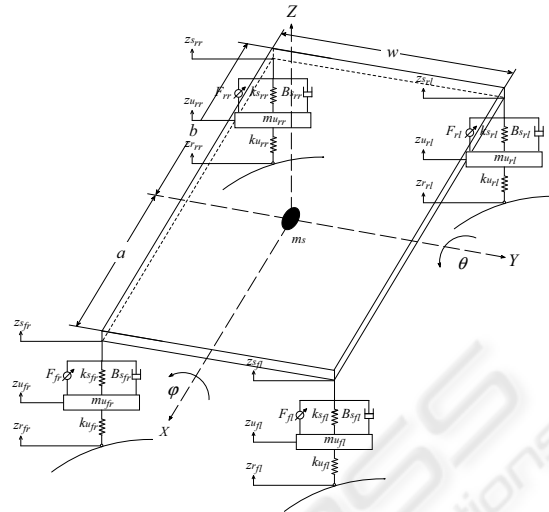


Figure 1: Full-vehicle suspension model.

where the followings parameters and variables are taken which respect to the static equilibrium position (Ikenaga, Lewis, Campos, Davis, 2000):

- ms is sprung mass $[kg]$,
- mu is unsprung mass $[kg]$,
- Ks_{fl} is front-left suspension spring stiffness $[N/m]$,
- Ks_{fr} is front-right suspension spring stiffness $[N/m]$,
- Ks_{rl} is rear-left suspension spring stiffness $[N/m]$,
- Ks_{rr} is rear-right suspension spring stiffness $[N/m]$,
- Bs_{fl} is front-left suspension damping $[N/m/s]$,
- Bs_{fr} is front-right suspension damping $[N/m/s]$,
- Bs_{rl} is rear-left suspension damping $[N/m/s]$,
- Bs_{rr} is rear-right suspension damping $[N/m/s]$,
- Ku_{fl} is tire-left spring stiffness $[N/m]$,
- Ku_{fr} is tire-right spring stiffness $[N/m]$,
- Ku_{rl} is tire-left spring stiffness $[N/m]$,
- Ku_{rr} is tire-right spring stiffness $[N/m]$,
- a is length between front of vehicle and center of gravity of sprung mass $[m]$,
- b is length between rear of vehicle and center of gravity of sprung mass $[m]$,
- w is width of sprung mass $[m]$,
- I_{xx} is roll axis moment of inertia $[kg \cdot m^2]$,
- I_{yy} is pitch axis moment of inertia $[kg \cdot m^2]$,

- F_{fl} is force at the front-left suspension [N],
- F_{fr} is force at the front-right suspension [N],
- F_{rl} is force at the rear-left suspension [N],
- F_{rr} is force at the rear-right suspension [N],
- Zr_{fl} is terrain disturbance heights at the front-left wheel [m],
- Zr_{fr} is terrain disturbance heights at the front-right wheel [m],
- Zr_{rl} is terrain disturbance heights at the rear-left wheel [m],
- Zr_{rr} is terrain disturbance heights at the rear-right wheel [m],
- g is the constant of graveness in the terrestrial surface, $9.80665 [m/s^2]$.

In this model, the car body is represented as a *sprung mass*, and the wheels are represented as an *unsprung mass* connected to the ground via the tire spring. The tire is an *undamped spring* between the axle and the ground. The suspension consists of passive dampers in parallel with four actuators and four springs.

2.2 Actuators

The suspension actuators are taken to be a force actuator acting between the car body and the axle of the car. The chosen *ServoRam^{TM2}* actuator, depicted in Fig. 2, produces an electromagnetic force and a pneumatic force acting simultaneously on the same output element. This electromagnetic actuator has zero mechanical hysteresis, since the force is applied directly to the output element. It has zero electrical hysteresis because a microamp in one direction produces a positive force, and a microamp in the opposite direction produces a negative force, so that the force output is an exactly linear function of the current input. A linear transducer measures the position of the piston. The small control time constant allows the force to be changed at a rate of thousands of Newtons per millisecond, so the suspension system can instantly adapt to every road condition. These linear motors consists of just two parts: the fixed stator and the moveable slider. These two parts are not connected by slip rings or by cables. Since the linear stroke directly without the use of mechanical gears, belts or ball screws, there is no wear or mechanical play. In a practical point of view, the ram is placed between the wheel

point (on the vehicle chassis) and the wheel stub axle, so as to carry all the vertical forces, see Fig. 3. The forces transferred from the wheel to the chassis may be precisely controlled by the electromagnetic forces. A force-measuring transducer may be used to control the current to the coil system, so as to maintain the total upward force at a constant value, irrespective of the wheel vertical motion. The desired value of this constant force may be determined in turn by the output from a wheel-point accelerometer, so as to hold the vehicle steady against pitch and roll motions, for example.

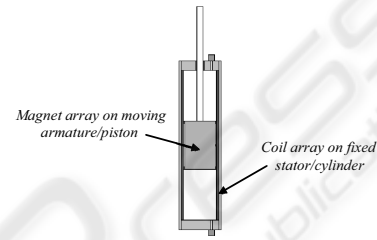


Figure 2: Simplified schematic of the *ServoRamTM* actuator.

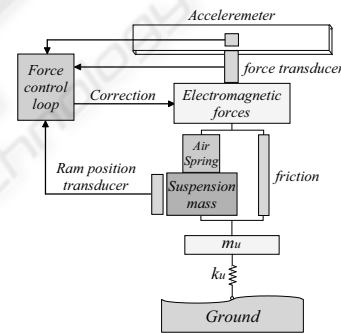


Figure 3: *ServoRamTM* actuator system for active suspension.

3 STATE SPACE-MODEL

The governing equations of this system are presented considering the following state variables (Ikenaga, Lewis, Campos, Davis, 2000):

- $x_1 = z$ is the heave position (ride height of sprung mass),
- $x_2 = \dot{z}$ is the heave velocity (payload velocity of sprung mass),
- $x_3 = \theta$ is the pitch angle,
- $x_4 = \dot{\theta}$ is the pitch angular velocity,
- $x_5 = \phi$ is the roll angle,
- $x_6 = \dot{\phi}$ is the roll angular velocity,

²Name applied to the AMT® ram technology, and all AMT® electromagnetic rams are, in fact, *ServoRamTM*. This technology has been developed over the last 10 years by AMT's Chief Scientist, Phillip Denne.

- $x_7 = Z_{u_{fl}}$ is the front-left wheel unsprung mass height,
- $x_8 = \dot{Z}_{u_{fl}}$ is the front-left wheel unsprung mass velocity,
- $x_9 = Z_{u_{fr}}$ is the front-right wheel unsprung mass height,
- $x_{10} = \dot{Z}_{u_{fr}}$ is the front-right wheel unsprung mass velocity,
- $x_{11} = Z_{u_{rl}}$ is the rear-left wheel unsprung mass height,
- $x_{12} = \dot{Z}_{u_{rl}}$ is the rear-left wheel unsprung mass velocity,
- $x_{13} = Z_{u_{rr}}$ is the rear-right wheel unsprung mass height,
- $x_{14} = \dot{Z}_{u_{rr}}$ is the rear-right wheel unsprung mass velocity,

Linear differential equations that describe the dynamics can be formulated as:

$$\begin{aligned}
 \dot{x}_1 &= x_2 \\
 \dot{x}_2 &= (F_{fl} + F_{fr} + F_{rl} + F_{rr} - (K_{s_{fl}} + K_{s_{fr}} + K_{s_{rl}} + K_{s_{rr}})) \cdot x_1 - (B_{s_{fl}} + B_{s_{fr}} + B_{s_{rl}} + B_{s_{rr}}) \cdot x_2 + (a \cdot (K_{s_{fl}} + K_{s_{fr}}) - b \cdot (K_{s_{rl}} + K_{s_{rr}})) \cdot x_3 + (a \cdot (B_{s_{fl}} + B_{s_{fr}}) - b \cdot (B_{s_{rl}} + B_{s_{rr}})) \cdot x_4 + K_{s_{fl}} \cdot x_7 + B_{s_{fl}} \cdot x_8 + K_{s_{fr}} \cdot x_9 + B_{s_{fr}} \cdot x_{10} + K_{s_{rl}} \cdot x_{11} + B_{s_{rl}} \cdot x_{12} + K_{s_{rr}} \cdot x_{13} + B_{s_{rr}} \cdot x_{14} / ms - g \\
 \dot{x}_3 &= x_4 \\
 \dot{x}_4 &= (-a \cdot (F_{fl} + F_{fr}) + b \cdot (F_{rl} + F_{rr}) + (a \cdot (K_{s_{fl}} + K_{s_{fr}}) - b \cdot (K_{s_{rl}} + K_{s_{rr}})) \cdot x_1 + (a \cdot (B_{s_{fl}} + B_{s_{fr}}) - b \cdot (B_{s_{rl}} + B_{s_{rr}})) \cdot x_2 - (a^2 \cdot (K_{s_{fl}} + K_{s_{fr}}) + b^2 \cdot (K_{s_{rl}} + K_{s_{rr}})) \cdot x_3 - (a^2 \cdot (B_{s_{fl}} + B_{s_{fr}}) + b^2 \cdot (B_{s_{rl}} + B_{s_{rr}})) \cdot x_4 - a \cdot K_{s_{fl}} \cdot x_7 - a \cdot B_{s_{fl}} \cdot x_8 - a \cdot K_{s_{fr}} \cdot x_9 - a \cdot B_{s_{fr}} \cdot x_{10} + b \cdot K_{s_{rl}} \cdot x_{11} + b \cdot B_{s_{rl}} \cdot x_{12} + b \cdot K_{s_{rr}} \cdot x_{13} + b \cdot B_{s_{rr}} \cdot x_{14}) / I_{yy}
 \end{aligned} \tag{1}$$

$$\begin{aligned}
 \dot{x}_5 &= x_6 \\
 \dot{x}_6 &= ((F_{fl} - F_{fr} + F_{rl} - F_{rr}) - \frac{w}{2} \cdot ((K_{s_{fl}} + K_{s_{fr}} + K_{s_{rl}} + K_{s_{rr}}) \cdot x_5 + (B_{s_{fl}} + B_{s_{fr}} + B_{s_{rl}} + B_{s_{rr}})) \cdot x_6 + K_{s_{fl}} \cdot x_7 + B_{s_{fl}} \cdot x_8 - K_{s_{fr}} \cdot x_9 - B_{s_{fr}} \cdot x_{10} + K_{s_{rl}} \cdot x_{11} + B_{s_{rl}} \cdot x_{12} - K_{s_{rr}} \cdot x_{13} + B_{s_{rr}} \cdot x_{14}) / (2 \cdot w / I_{xx}) \\
 \dot{x}_7 &= x_8 \\
 \dot{x}_9 &= x_{10} \\
 \dot{x}_{10} &= (-F_{fr} + K_{s_{fr}} \cdot x_1 + B_{s_{fr}} \cdot x_2 - a \cdot K_{s_{fr}} \cdot x_3 - a \cdot B_{s_{fr}} \cdot x_4 - \frac{w}{2} \cdot K_{s_{fr}} \cdot x_5 - \frac{w}{2} \cdot B_{s_{fr}} \cdot x_6 - (K_{u_{fr}} + K_{s_{fr}}) \cdot x_9 - B_{s_{fr}} \cdot x_{10} + K_{u_{fr}} \cdot Z_{r_{fr}}) / mu_{fr} - g \\
 \dot{x}_{11} &= x_{12} \\
 \dot{x}_{12} &= (-F_{rl} + K_{s_{rl}} \cdot x_1 + B_{s_{rl}} \cdot x_2 + b \cdot K_{s_{rl}} \cdot x_3 + b \cdot B_{s_{rl}} \cdot x_4 + \frac{w}{2} \cdot K_{s_{rl}} \cdot x_5 + \frac{w}{2} \cdot B_{s_{rl}} \cdot x_6 - (K_{u_{rl}} + K_{s_{rl}}) \cdot x_{11} - B_{s_{rl}} \cdot x_{12} + K_{u_{rl}} \cdot Z_{r_{rl}}) / mu_{rl} - g \\
 \dot{x}_{13} &= x_{14} \\
 \dot{x}_{14} &= (-F_{rr} + K_{s_{rr}} \cdot x_1 + B_{s_{rr}} \cdot x_2 + b \cdot K_{s_{rr}} \cdot x_3 + b \cdot B_{s_{rr}} \cdot x_4 - \frac{w}{2} \cdot K_{s_{rr}} \cdot x_5 - \frac{w}{2} \cdot B_{s_{rr}} \cdot x_6 - (K_{u_{rr}} + K_{s_{rr}}) \cdot x_{13} - B_{s_{rr}} \cdot x_{14} + K_{u_{rr}} \cdot Z_{r_{rr}}) / mu_{rr} - g
 \end{aligned} \tag{2}$$

This system can be summarized by the following linear space-state representation:

$$\begin{aligned}
 \dot{x}(t) &= A \cdot x(t) + B \cdot u(t) + B_p \cdot u_p(t) \\
 y(t) &= C \cdot x(t),
 \end{aligned} \tag{3}$$

where:

- $x \in \mathfrak{R}^{14 \times 1}$ is the system state vector,
- $u \in \mathfrak{R}^{4 \times 1}$ is a vector composed of the control forces. $u = [F_{fl} \ F_{fr} \ F_{rl} \ F_{rr}]^T$,
- $u_p \in \mathfrak{R}^{5 \times 1}$ is a vector whose components are the disturbance inputs. $u_p = [g \ Z_{r_{fl}} \ Z_{r_{fr}} \ Z_{r_{rl}} \ Z_{r_{rr}}]^T$,
- $y \in \mathfrak{R}^{3 \times 1}$ is the system output vector. $y = [Z \ \theta \ \phi]^T$,
- $A, B, B_p,$ and C are constant matrices of appropriate dimensions.

4 CONTROLLER MODEL

The controller design considers:

- Control loops that stabilize heave, pitch and roll responses,

- Input decoupling transformation that blends the inner and outer control loops allowing streamlined design yet gives performance better than over-simplified decoupled techniques.

By employing a state observer, the full state feedback is available for the entire vehicle, and pitch angle is inferred from a combination of rate sensors and accelerometers. The control law \bar{u} is computed by a state feedback associated with the integral of the tracking error: $\bar{u} = -[K_1 \ K_2] \cdot [x \ q]^T = -K \cdot \bar{x}$; K_1 and K_2 are computed according to Eq.4. This controller design is illustrated in Fig.4.

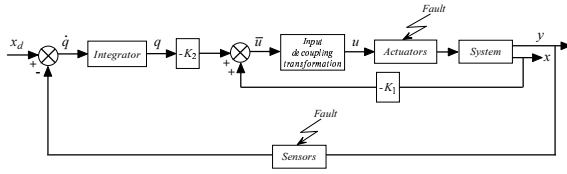


Figure 4: Controller block diagram.

The control procedure can be briefly summarized as follows: Let us consider the following optimization problem.

The performance index to be minimized is:

$$J = \frac{1}{2} \cdot \int_0^{\infty} [\bar{x}^T(t) \cdot Q \cdot \bar{x}(t) + \bar{u}^T(t) \cdot R \cdot \bar{u}(t)] dt, \quad (4)$$

where:

- $\bar{x} \in \mathfrak{R}^{17 \times 1}$ is the augmented system state vector. $\bar{x} = [x^T \ q^T]^T$,
- $\bar{u} \in \mathfrak{R}^{3 \times 1}$ is a vector whose components are the control forces, provided by the actuators, for heave (F_z), pitch (F_θ) and roll (F_ϕ),
- $Q \in \mathfrak{R}^{17 \times 17}$ is positive semi-definite matrix,
- $R \in \mathfrak{R}^{3 \times 3}$ is tuning diagonal matrix.

The good performance of the suspension system is related to the minimization of the term $\bar{x}^T \cdot Q \cdot \bar{x}$ and an adequate choice of R , because the comfort depends of the term $\bar{u}^T \cdot R \cdot \bar{u}$. The optimal control strategy that minimizes the cost function was found to be $\bar{u}(t) = -K \cdot \bar{x}(t)$, where the gain matrix K can be computed by solving an algebraic Riccati equation. So, a set of LQR optimal feedback gains corresponding to different weighting factors in the quadratic function J is chosen. The feedback control is designed to increase the relative damping of a particular mode of motion in the system by augmenting one or more of the coefficients of the equation of motion by actuating the control signals in response to motion feedback variables.

From Fig.1, the equivalent relationship between $F_z(t)$, $F_\theta(t)$ and $F_\phi(t)$, and the forces generated by the actuators can be defined by:

$$\begin{bmatrix} F_{fl}(t) \\ F_{fr}(t) \\ F_{rl}(t) \\ F_{rr}(t) \end{bmatrix} = \frac{1}{2} \begin{bmatrix} \frac{b}{(a+b)} & \frac{-1}{(a+b)} & \frac{1}{w} \\ \frac{b}{(a+b)} & \frac{-1}{(a+b)} & \frac{-1}{w} \\ \frac{a}{(a+b)} & \frac{1}{(a+b)} & \frac{1}{w} \\ \frac{a}{(a+b)} & \frac{1}{(a+b)} & \frac{-1}{w} \end{bmatrix} \cdot \begin{bmatrix} F_z(t) \\ F_\theta(t) \\ F_\phi(t) \end{bmatrix}, \quad (5)$$

Therefore the nominal control is given by:

$$\begin{bmatrix} F_z(t) \\ F_\theta(t) \\ F_\phi(t) \end{bmatrix} = -K \cdot \bar{x}(t), \quad (6)$$

where $K \in \mathfrak{R}^{3 \times 17}$.

5 FAULT ANALYSIS AND SIMULATION RESULTS

In the following simulations, the full-car suspension system was simulated for the input terrain disturbances $Zr(t)$ actuating between $2 \leq t \leq 8$ s:

$$Zr(t) = \begin{bmatrix} Zr_{fl}(t) \\ Zr_{fr}(t) \\ Zr_{rl}(t) \\ Zr_{rr}(t) \end{bmatrix} = \begin{bmatrix} 0.05 \cdot \sin(w \cdot t) \\ 0.15 \cdot \sin(w \cdot t) \\ 0.05 \cdot \sin(w \cdot (t + \tau)) \\ 0.15 \cdot \sin(w \cdot (t + \tau)) \end{bmatrix}, \quad (7)$$

where:

- $\omega = 9$ [rad/s], is the terrain disturbance frequency,
- $\tau = 0.1409$ [s], is the time delay given by: $\tau = L/v = (a+b)/v$,
- L is the distance between the front and rear axles of the vehicle [m],
- $v = 22$ [m/s], is the speed at which the vehicle travels.

The given initial conditions are $\bar{x} = 0$, and the required torque to be delivered by the actuators is determined as in fault-free cases. The objective here is to analyze the effects of a sensor- and actuator-faults on the active suspension.

5.1 Sensor Fault

At $t = 5.5$ s a sensor fault occurs in the second sensor measuring θ . This fault corresponds to a bias equal

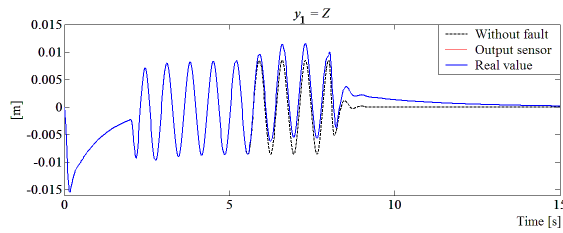


Figure 5: y_1 : Heave position (ride height of sprung mass).

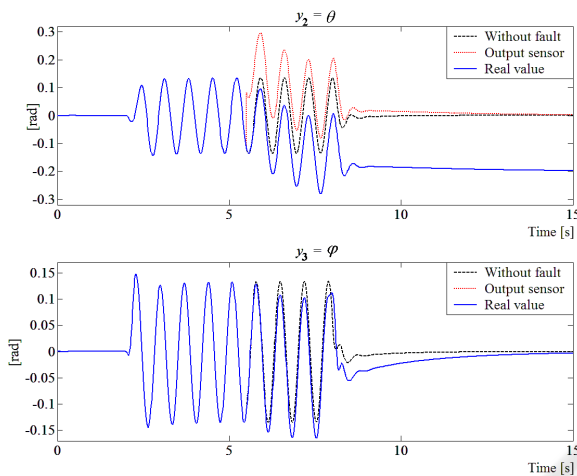


Figure 6: (a) y_2 : Pitch angle; (b) y_3 : Roll angle.

to 0.2 rad . Due to this fault, similar real value θ is shifted of -0.2 rad from the output sensor which goes to its reference value. The real value of θ is far from its reference because the control input naturally reacts in the presence of the sensor fault. Figs. 5 and 6 show that the other outputs Z and φ are also affected by this fault but reach their reference value again.

The increase of the necessary force that should be applied to the actuators in front of this default is depicted in Figs. 7 and 8. Fig. 7(a) illustrates a saturation ($\pm 20000 \text{ [N]}$) reached in the actuator, in the presence of this fault. Figs. 7(b) and 8 show the other influence of this sensor fault on the control input.

5.2 Actuator Fault

Other experiments simulating actuator faults are performed. At $t = 5.5 \text{ [s]}$, a reduction of 75% in the second actuator effectiveness (F_{fr}) is simulated. Figs. 9 to 12. illustrate simulation results. Figs. 9 and 10 show the permanent shift between the outputs with no fault and the outputs with fault. This shift is due to the fact that the other control inputs are affected by the fault due to the closed-loop and coupling between each other. The new necessary forces that should be applied in the actuators to compensate this loss of

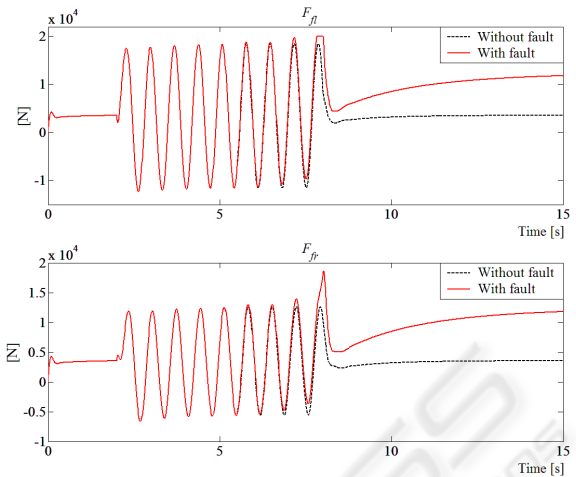


Figure 7: (a) F_{fl} : Force at the front-left suspension; (b) F_{fr} : Force at the front-right suspension.

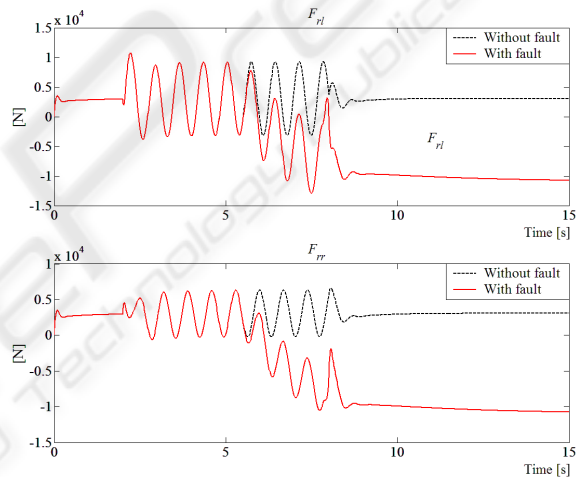


Figure 8: (a) F_{rl} : Force at the rear-left suspension; (b) F_{rr} : Force at the rear-right suspension.

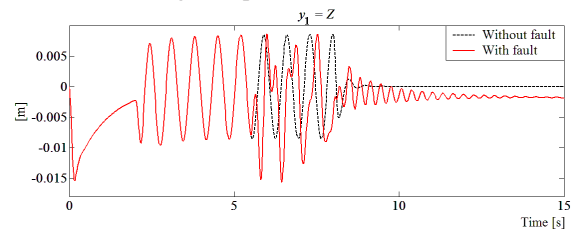


Figure 9: y_1 : Heave position (ride height of sprung mass).

effectiveness are shown in Figs. 11 and 12. These force increases do not surpass the maximum allowable force limits in the actuators.

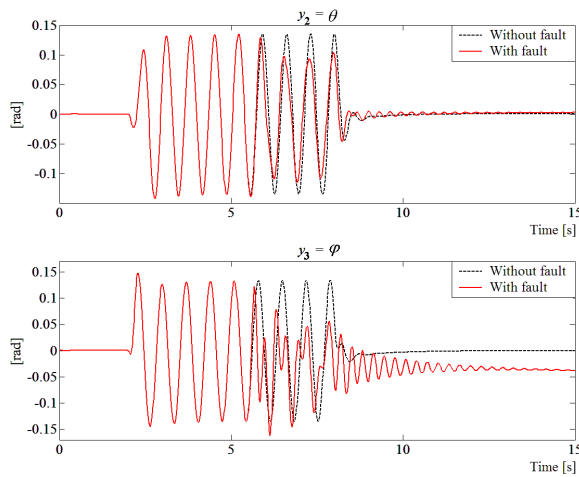


Figure 10: (a) y_2 : Pitch angle; (b) y_3 : Roll angle.

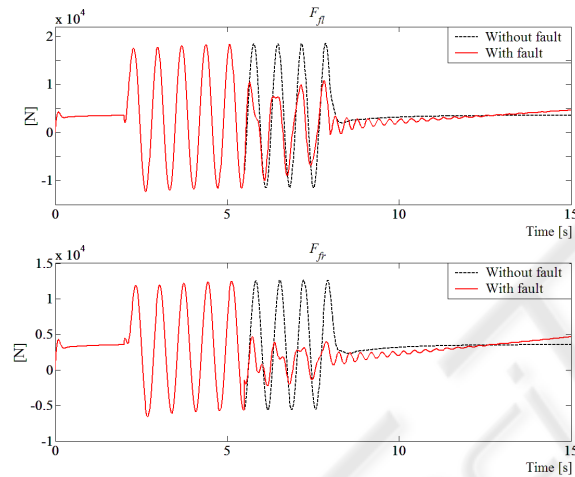


Figure 11: (a) F_{fl} : Force at the front-left suspension; (b) F_{fr} : Force at the front-right suspension.

6 CONCLUSIONS AND FUTURE WORK

In this paper, it was shown that active suspension can improve all three performance aspects *i.e.* passenger ride comfort, handling, and rattle space.

A nominal control law is designed for this active suspension system and the effect of the profile of the road is analyzed in the first part. The main aim of this work is the study of the influence of sensor and actuator faults on the control law.

The obtained results are realistic and show the importance of the design of a fault tolerant control system (FTCS) able to compensate this kind of fault. This work is just starting. Future work will also take into account the loss of a complete sensor or actuator in order to preserve safety and passengers' comfort.

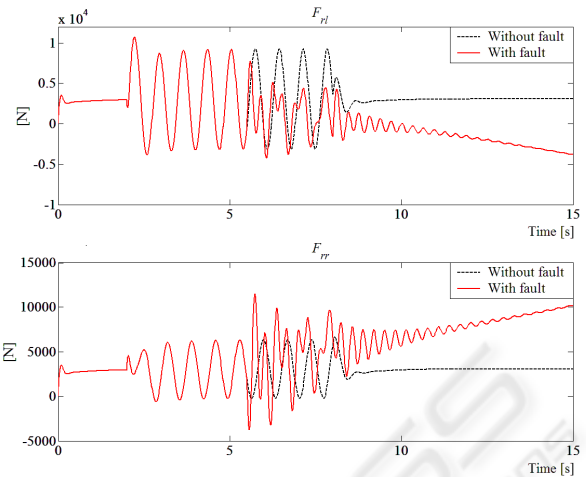


Figure 12: (a) F_{rl} : Force at the rear-left suspension; (b) F_{rr} : Force at the rear-right suspension.

ACKNOWLEDGEMENTS

This work was possible thanks to the support of DI-CYT – Universidad de Santiago de Chile, USACH, through Project 0607UO and Project 0607JD.

REFERENCES

- Buckner G., Schuetze K., Beno J.: Active Vehicle Suspension Control Using Intelligent Feedback Linearization. American Control Conference, Chicago, Illinois, USA (2000) 4019–4024
- Fukao T., Yamawaki A., Adachi N.: Nonlinear and H_∞ Control of Active Suspension Systems with Hydraulic Actuators. American Control Conference, Chicago, Illinois, USA (2000) 5125–5128
- Giua A., Seatzu C., Usai G.: Active Axletree Suspension for Road Vehicles with Gain-Switching. 39th IEEE Conference on Decision and Control Sydney Convention and Exhibition Centre, Sydney, Australia (2000)
- Lefebvre D., Chevrel P., Richard S.: A Hinfinity-based control design methodology dedicated to active control of vehicle longitudinal oscillations. 40th IEEE Conference on Decision and Control Orlando, Florida, USA (2001) 99–104
- Lakehal-Ayat M., Diop S., Fenaux E.: Development of a Full Active Suspension System. 15th Triennial World Congress IFAC, Barcelona, Spain (2002)
- Karlsson N., Teely A., Hrovatz D.: A Backstepping Approach to Control of Active Suspensions. 40th IEEE Conference on Decision and Control Orlando, Florida, USA (2001) 4170–175
- Alleyne A., Hedrick J.: Nonlinear Adaptive Control of Active Suspensions. IEEE Trans. Control Syst. Technol. 1 (1995) 94–101

- Engelman G., Rizzon G.: Including the Force Generation Process in Active Suspension Control Formulation. American Control Conference, San Francisco, California, USA (1993)
- Alleyne A., Liu R., Wright H.: On the Limitations of Force Tracking Control for Hydraulic Active Suspensions. American Control Conference, Philadelphia, USA (1998) 43–47
- Noura H., Theilliol D., Sauter D.: Actuator Fault-Tolerant Control Design: Demonstration on a Three-Tank-System. International Journal of Systems Science series 9 (2000) 1143–1155
- Zhang Y., Jiang J.: Design of Restructurable Active Fault-Tolerant Control Systems. 15th Triennial World Congress IFAC, Barcelona, Spain (2002)
- Ikenaga S., F. Lewis, Campos J., Davis L.: Active Suspension Control of Ground Vehicle Based on a Full-Vehicle Model. American Control Conference, Chicago, Illinois, USA (2000) 4019–4024



Scitec Press
Science and Technology Publications